

1 **Title:**

2 Proliferation maintains the undifferentiated status of stem cells: the role of the planarian cell cycle  
3 regulator Cdh1.

4

5 **Authors:**

6 Yuki Sato<sup>1</sup>, Yoshihiko Umesono<sup>2</sup>, Yoshihito Kuroki<sup>4,5</sup>, Kiyokazu Agata<sup>4</sup>, Chikara Hashimoto<sup>1,3</sup>

7

8 **Affiliations:**

9 <sup>1</sup>JT Biohistory Research Hall, Japan

10 <sup>2</sup>Graduate School of Life Science, University of Hyogo, Japan

11 <sup>3</sup>Department of Biology, Graduate School of Science, Osaka University, Japan

12 <sup>4</sup>Laboratory of Regeneration Biology, National Institute for Basic Biology, Japan

13 <sup>5</sup>Department of Basic Biology, School of Life Science, The Graduate University for Advanced  
14 Studies, SOKENDAI, Japan

15

16 **ORCID:**

17 Yuki Sato: 0000-0002-3758-3452

18 Yoshihiko Umesono: 0000-0003-0851-2003

19 Yoshihito Kuroki: 0000-0001-7717-8147

20 Kiyokazu Agata: 0000-0002-5195-2576

21 Chikara Hashimoto: 0000-0002-1240-0410

22

23 **Corresponding author:**

24 Chikara Hashimoto

25 JT Biohistory Research Hall, 1-1 Murasaki-cho, Takatsuki, Osaka 569-1125, Japan.

26 E-mail: hashimoto@brh.co.jp

27

28 **Key words:** stem cells, differentiation, cell cycle, competence, planarian

29

30 **Summary statement:**

31 By using planarians, which have quite simple cell cycle regulation, we revealed that stem cells with  
32 cell cycle progression could not undergo differentiation even though an induction signal was  
33 activated.

34

35 **Abstract:**

36 The coincidence of cell cycle arrest and differentiation has been described in a wide variety of  
37 stem cells and organisms for decades, but the causal relationship is still unclear due to the  
38 complicated regulation of the cell cycle. Here, we used the planarian *Dugesia japonica* since it  
39 possesses a quite simple cell cycle regulation in which *cdh1* is the only factor that arrests the cell  
40 cycle. When *cdh1* was functionally inhibited, the planarians could not maintain their tissue  
41 homeostasis and could not regenerate their missing body parts. While the ablation of *cdh1* caused  
42 pronounced propagation of the stem cells, the progenitor and differentiated cells were decreased.  
43 Further analysis indicated that the stem cells without *cdh1* expression did not undergo differentiation  
44 even though they received ERK signaling activation as an induction signal. These results suggested  
45 that stem cells could not acquire differentiation competence without cell cycle arrest. Thus, we  
46 propose that cell cycle regulation determines the differentiation competence and that cell cycle exit  
47 to G0 enables stem cells to undergo differentiation.

48

## 49 **Introduction**

50 Stem cells, including fertilized eggs, embryonic stem cells (ESCs), hematopoietic stem cells  
51 (HSCs), myoblasts and fibroblasts, have the ability of self-renewal and differentiation. Excessive  
52 differentiation causes the depletion of stem cells, and excessive proliferation causes carcinogenesis.  
53 Therefore, the precise balance of proliferation and differentiation is required for development,  
54 homeostatic tissue turnover and regeneration. It has been proposed that “induction” is primarily  
55 responsible for differentiation. For example, BMP-4 is required for epidermal differentiation of  
56 undifferentiated ectoderm (animal cap) cells in *Xenopus* early development (Sasai and De Robertis,  
57 1997). The differentiation of sympathetic neurons from PC12 cells requires sustained ERK activation  
58 (Marshall, 1995; Avraham and Yarden, 2011). The activation of ERK signaling is also required for exit  
59 from pluripotency and for lineage commitment of mouse ESCs (Kunath et al., 2007; Stavridis et al.,  
60 2007). These reports emphasize the importance of induction signals to regulate the differentiation of  
61 stem cells. At the same time, the importance of “competence”, which is the capability to respond to  
62 induction signals has been proposed. For example, though the blastula animal cap cells of *Xenopus*  
63 have the ability to be induced by activin treatment to become mesoderm, the cap cells excised from  
64 the gastrula have lost this ability. Thus, both the extrinsic induction signals and the intrinsic  
65 competence are thought to be necessary for differentiation and they may function in parallel.

66 Meanwhile, it has been shown that the fate decision of stem cells such as myoblasts and  
67 embryonal carcinoma cells (ECCs) is made at the G1 phase (Nadal-Ginard, 1978; Wells, 1982).  
68 Notably, MyoD has already been present in proliferating myoblasts and bound to the regulatory region  
69 of its target genes, but the transcription is initiated only when the cell cycle is arrested (Skapek et al.,  
70 1995). Furthermore, human ESCs initiate the expression of marker genes for each germ layer at G1  
71 phase, and the epigenetic status of these genes becomes bivalent at G1 (Pauklin and Vallier, 2013;  
72 Singh et al., 2015). These reports suggest that there is a mutual relationship between the cell cycle and

73 differentiation, though the causal relationship remains to be clarified.

74       Cells decide whether to progress through or arrest their cell cycle during G1 phase. This decision  
75 depends on the level of cyclin-dependent kinase (CDK) activity. The CDK activity level becomes the  
76 lowest from late M phase to early G1 phase due to the degradation of Cyclins, and subsequent S phase  
77 entry requires the elevation of CDK activity. Especially, a ubiquitin E3-ligase, APC/C-Cdh1, is  
78 responsible for Cyclin degradation from the onset of G1 phase. To elevate the CDK activity for cell  
79 cycle progression, Cdh1 should be inactivated by binding of Emi1 or degraded through SCF-Skp2-  
80 mediated polyubiquitination. Therefore, the inactivation of APC/C-Cdh1 has been reported as a  
81 commitment point for progression through the cell cycle (Cappel et al., 2016). On the other hand, the  
82 sustained suppression of CDK activity induces cell cycle arrest at G1 phase. In addition to APC/C-  
83 Cdh1, CDK inhibitors (CKIs) such as INK family (p15, p16, p18 and p19) and CIP/KIP family (p21,  
84 p27 and p57) proteins inhibit CDK activity during G1 phase by direct binding. Furthermore, many  
85 other cell cycle regulators mutually interact with each other and construct a complicated network to  
86 regulate the cell cycle.

87       Previously, it was suggested that maintaining the proliferative state is important for the  
88 undifferentiated status of neural crest cells and lens placodal cells in *Xenopus* (Nagatomo and  
89 Hashimoto, 2007; Murato and Hashimoto, 2009), suggesting that cells tend to undergo differentiation  
90 once their cell cycle is arrested. If this is true, the cell cycle should be strictly regulated during  
91 development. It is known that cells can transiently arrest their cell cycle but can then proliferate again  
92 by restoring CDK activity during the developmental process. Such transient arrest makes cell cycle  
93 regulation highly dynamic. Since differentiation occurs at various times and places simultaneously  
94 during normal development in most multicellular organisms, complex and dynamic conversion of the  
95 cell cycle state seems to occur several times in the course of development. This is a major reason why  
96 investigation of the relationship between the cell cycle and differentiation has been problematic so far.

97 Planarians are well-known organisms that can regenerate any missing body part even from a  
98 tiny body fragment within a week. The remarkable regenerative ability is dependent on their adult  
99 stem cells called neoblasts (Agata and Watanabe, 1999; Newmark and Sánchez Alvarado, 2002). Since  
100 the neoblasts include pluripotent stem cells (PSCs), they give rise to all cell types in the planarian body,  
101 including germ-line cells (Shibata et al., 2010; Roberts-Galbraith and Newmark, 2015). By using the  
102 neoblasts, planarians also undergo perpetual tissue turnover throughout their life (Newmark and  
103 Sánchez Alvarado, 2000). The neoblasts are the only mitotic cells in the planarian body, and the cells  
104 never proliferate once they undergo differentiation. For this reason, planarian differentiation can be  
105 regarded as a kind of terminal differentiation. Since chemical inhibitors of ERK signaling and  
106 knockdown of the *erk-A* gene prohibit the differentiation of the neoblasts, the activation of ERK  
107 signaling is suggested to be responsible for the onset of differentiation as an induction signal (Tasaki  
108 et al., 2011a). Furthermore, planarians are one of the most basal organisms possessing three germ  
109 layers and three body axes, and are located at the branching point of protostomes and deuterostomes  
110 in the phylogenetic tree. Thus, universal features among multicellular organisms should have been  
111 acquired at planarians and conserved from them onwards.

112 Recently, genome analysis of multiple planarian species revealed that planarians have lost 124  
113 genes essential for mice or humans (Grohme et al., 2018). *cdkn1b* encoding p27, a CIP/KIP family  
114 CKI, was one of the lost genes in planarians. It has also been reported that *cdkn1a* encoding p21 was  
115 not found in the genome of a European planarian, *Schmidtea mediterranea* (Pearson and Alvarado,  
116 2010). Consistently, we could not find any CKI genes, including INK family and CIP/KIP family  
117 genes, in a draft genome of a freshwater planarian, *Dugesia japonica* (An et al., 2018). While most  
118 known factors regulating cell cycle arrest were not found in planarians, we found a *cdh1* gene (Fig.  
119 S1). Therefore, it could be thought that determination of whether cells arrest their cell cycle or enter  
120 the next round of cell division in planarians primarily depends on the presence or absence of Cdh1

121 expression. Interestingly, we also could not find Cdh1 inactivator genes *emil* and *skp2* in the planarian  
122 genome. Taking these findings altogether, it is suggested that planarian cells cannot proliferate in the  
123 presence of Cdh1. Thus, it is possible to think that planarian species have a quite simple strategy for  
124 cell cycle regulation which is easy to manipulate by focusing only on *cdh1* expression. Furthermore,  
125 the neoblasts are the only proliferative cells in the planarian body, which enables us to focus on the  
126 cell cycle and differentiation of the neoblasts without any unintended effects on the other cells.  
127 Collectively, these considerations make planarians an ideal model for studying the relationship  
128 between the cell cycle and differentiation of stem cells.

129 In this study, we used *D. japonica* and showed that the ablation of planarian *cdh1* caused a  
130 drastic increase of the neoblasts, while the progenitor and differentiated cells were decreased.  
131 Moreover, the neoblasts without *cdh1* expression did not undergo differentiation, whereas ERK  
132 signaling was definitely activated in the course of regeneration. Based on these results, we propose a  
133 universal trait of stem cells that could be conserved among multicellular organisms: the cell cycle  
134 determines competence toward induction signals and only the stem cells arresting their cell cycle  
135 undergo differentiation according to the surroundings. This is the first report clearly showing that stem  
136 cells with cell cycle progression do not undergo differentiation even though they receive an induction  
137 signal.

138

139 **Results**

140 ***cdh1* was expressed in the differentiating cells**

141 While “induction” has attracted much attention, the importance of “competence” for  
142 differentiation has also been suggested for a long time. Accumulating evidence indicates that cell cycle  
143 arrest induces differentiation of stem cells (Lange and Calegari, 2010), but whether the cell cycle  
144 progression directly involves the repression of differentiation and maintenance of the undifferentiated  
145 state has been unclear. To investigate the relationship between the cell cycle and differentiation, we  
146 focused on the planarian *cdh1* gene, since it could be possible that *cdh1* plays a pivotal role in the  
147 decision of cell cycle arrest in planarians. Whole-mount in situ hybridization (WISH) revealed that  
148 *cdh1* was expressed in all body regions except the margin and pharynx (Fig. 1A). To examine whether  
149 the neoblasts expressed *cdh1*, we conducted double-WISH of *cdh1* and a neoblast marker gene, *piwiA*,  
150 (Yoshida-Kashikawa et al., 2007; Hayashi et al., 2010; Shibata et al., 2010). As a result, we observed  
151 that a fraction of the cells co-expressed *cdh1* and *piwiA* (Fig. 1B, white arrows) but we also observed  
152 single-positive cells of *cdh1* (Fig. 1B, black arrowheads) and *piwiA* (Fig. 1B, white arrowheads).  
153 Further, we examined the expression of *cdh1* during regeneration. WISH at 3 days post-amputation  
154 (dpa) revealed that *cdh1* was also expressed within the blastema region (Fig. 1C). Since the blastema  
155 region was formed by differentiating cells (*piwiA* mRNA negative/ PiwiA protein positive; Tasaki et  
156 al., 2011a), it is suggested that the *cdh1* was expressed in the committed neoblasts and differentiating  
157 cells. Based on these results and the known function of *cdh1*, planarian *cdh1* may be involved in cell  
158 cycle arrest in the differentiating cells.

159

160 ***cdh1* knockdown planarians showed disruption of homeostatic tissue turnover and blastema**  
161 **formation**

162 To evaluate the function of *cdh1* in planarians, we conducted functional inhibition by feeding

163 RNAi. We fed planarians dsRNA-containing food on 4 successive days from day 1 and once on day  
164 8, and observed their phenotype at day 17 (Fig. 1D). Although the control animals maintained the  
165 normal body without any tissue disorder, some *cdhl* knockdown (KD) planarians had an epithelium  
166 disorder (8/30) or more severe headless phenotype (6/30), although the half of them (15/30) appeared  
167 normal (Fig. 1E). However, while the transverse section of the control animals showed normal  
168 morphology of the intestine, that of *cdhl* KD animals was collapsed even though the external  
169 morphology of the animals looked intact (Fig. 1F). Since planarians continuously undergo rapid tissue  
170 turnover, it is possible to think that the disruption of tissue homeostasis was caused by an insufficient  
171 supply of differentiated cells from the neoblasts.

172 We also examined the regeneration of *cdhl* KD animals after head and tail amputation at day  
173 12 (Fig. 1G). The control animals formed blastemas normally and were regenerating their head and  
174 tail at 3 dpa. Notably, the head blastema of control animals was already regenerating eyes. On the  
175 other hand, more than half of *cdhl* KD animals (6/10) could not form blastemas, and the others had  
176 already died at 3 dpa (Fig. 1H). Finally, the control animals completely regenerated their missing body  
177 parts (4/4), but *cdhl* KD animals could not regenerate at all (3/4) at 7 dpa. Since blastema formation  
178 is the process that occurs subsequent to wound closure, we examined the wound healing response of  
179 *cdhl* KD animals by making an incision instead of amputation. In contrast to blastema formation,  
180 wound closure successfully occurred in 1 day both in control and in *cdhl* KD planarians, and JNK  
181 inhibitor SP600125 disturbed the wound closure, as previously described (Fig. S2; Tasaki et al., 2011b).  
182 This result indicated that the failure of blastema formation in *cdhl* KD animals was not a result of  
183 disruption of wound closure. Thus, it could be thought that the differentiating cells that form the  
184 blastema were not supplied in *cdhl* KD animals.

185 The disruption of tissue homeostasis and blastema formation both suggested that differentiated  
186 cells were not supplied sufficiently in *cdhl* KD animals. Such absence of differentiated cells could be



187 explained by either the ablation of the neoblasts or the disruption of the differentiation process.

188

### 189 **The neoblasts were highly propagated in *cdh1* knockdown animals**

190 To clarify whether the *cdh1* KD animals maintained their neoblasts, we checked the expression  
191 of neoblast marker genes. WISH of *piwiA* and *tgs1*, a candidate PSC marker gene in neoblasts (Zeng  
192 et al., 2018), showed that control and *cdh1* KD animals were indistinguishable at day 7, but the *cdh1*  
193 KD animals showed intense expression of both genes throughout their body at day 17 (Fig. 2A, B).  
194 This result can be explained in two ways: higher gene expression or increased number of the neoblasts.  
195 Then, we attempted to examine whether the neoblasts were increased by comparison of the areas where  
196 the neoblasts were present. Section in situ hybridization (SISH) at day 17 revealed that the area  
197 expressing *piwiA* within the total mesenchymal area was 18.3% in control animals and 46.1% in *cdh1*  
198 KD animals (Fig. 2C, D). Correspondingly, the percentage of mesenchymal area expressing *tgs1* was  
199 1.98% in control animals and 16.3% in *cdh1* KD animals (Fig. 2C, D). The drastic increase of the area  
200 expressing neoblast marker genes indicated that the neoblasts were highly propagated in *cdh1* KD  
201 animals. Especially the area of PSCs (*tgs1*-positive cells) was more than 8.5 times larger.

202 In addition to the increase of the area expressing neoblast marker genes, the number of  
203 phosphorylated histone H3 (pH3)-positive M phase cells was also increased in *cdh1* KD animals by  
204 more than 2-fold compared to that in control animals at day 17 (Fig. 2E, F), though the signal intensity  
205 looked much higher. Because the neoblasts are the only proliferative cells in the planarian body, the  
206 increase of pH3-positive cells also indicated an increase of the neoblasts in *cdh1* KD animals. These  
207 results suggested that the disruptions of both homeostatic turnover and regeneration in *cdh1* KD  
208 animals were caused not by the ablation of neoblasts but by the disruption of the differentiation process.

209

210 **The neoblasts in *cdh1* KD animals did not undergo differentiation in homeostatic condition.**

211 The drastic propagation of the neoblasts in *cdh1* KD animals suggested that the collapse of tissue  
212 homeostasis was caused by disruption of the differentiation process. To assess the differentiation of  
213 the neoblasts, we examined the expression of progenitor and differentiated cell marker genes by RT-  
214 qPCR analysis (Fig. 3A). Consistent with the results of in situ hybridization, the expression levels of  
215 *piwiA* and *tgs1* in *cdh1* KD animals were not distinguishable from those in control animals at day 7,  
216 but they started to be increased at day 11 and reached almost 3-fold higher than those in control animals  
217 at day 17. The S phase marker genes *pcna*, *mcm2* and *mcm3* also showed 3-4 fold higher expression  
218 at day 17 in *cdh1* KD animals than in control animals (Fig. 3A, Fig. S3). Taken together with the  
219 increase of M phase marker pH3-positive cells, this suggested the active cell cycling and accumulation  
220 of the neoblasts without any cell cycle arrest. In contrast to the neoblast marker genes, the expression  
221 of epithelial progenitor marker gene *prog1* and differentiated intestine marker gene *inx1* in *cdh1* KD  
222 animals was decreased to half or less of that in control animals (Fig. 3A). This suggested that the  
223 progenitor and differentiated cells were decreased in *cdh1* KD planarians. Since simple propagation  
224 of the neoblasts would also cause an increase of progenitor and differentiated cells, the decline of the  
225 progenitor and differentiated cells indicated that the process of differentiation was disrupted.

226 We also confirmed the change of cell populations by FACS (fluorescent-activated cell sorting)  
227 using nuclear and cytoplasmic staining by Hoechst33342 and Calcein AM (Hayashi et al., 2006),  
228 which distinguish the neoblasts from the differentiated cells independently of marker gene expression.  
229 FACS analysis classified the planarian cells into 3 fractions (Fig. 3B): the X1 fraction showing high  
230 nuclear content and scant cytoplasm contains the neoblasts in S, G2 and M phase, the X2 fraction  
231 showing low nuclear content and scant cytoplasm contains the neoblasts in G1 phase and a part of the  
232 differentiated cells, and the Xis fraction showing low nuclear content and developed cytoplasm  
233 contains only differentiated cells (Hayashi et al., 2006). The *cdh1* KD animals showed a higher ratio  
234 of the X1 fraction than the control animals from day 7 to 17 (Fig. 3B, C), which suggested that the

235 enhancement of self-renewal by *cdhl* KD preceded the increase of neoblast marker gene expression  
236 at day 7. In contrast to the X1 fraction, the ratio of the Xis fraction became lower than that of the  
237 control at day 11, 14 and 17 (Fig. 3B, C). The total cell numbers of control and *cdhl* KD animals were  
238 comparable though the ratio between them was dynamically changed (Fig. S4), indicating that the  
239 neoblasts were propagated without differentiation while the differentiated cells were decreasing due  
240 to rapid tissue turnover. Of note, the density plot of *cdhl* KD animals showed a clear border between  
241 the X2 fraction and Xis fraction which could not be observed in that of control animals. It could be  
242 thought that the cells that were present between the X2 fraction and Xis fraction were differentiating  
243 progenitor cells. Therefore, the results also suggested the disappearance of differentiating progenitor  
244 cells while the neoblasts were propagated. The ratio of the X2 fraction was not so significantly changed  
245 from day 7 to day 17 (Fig. 3B, C). However, it could be thought that the differentiating cells  
246 disappeared while the neoblasts passing through G1 phase were increased within the X2 fraction,  
247 which made the X2 fraction seemingly unchanged.

248 For further understanding, we specifically labeled the neoblasts by EdU incorporation at day 12  
249 and examined their differentiation at day 15 (Fig. 3D, E). In the control animals, 29.3% of EdU positive  
250 mesenchymal cells were *piwiA* positive neoblasts and the other 70.7% of EdU positive cells that had  
251 lost *piwiA* expression were newly differentiated cells. On the other hand, 68.7% of EdU positive  
252 mesenchymal cells retained *piwiA* expression in *cdhl* KD animals. This result clearly indicated that  
253 functional inhibition of *cdhl* suppressed the differentiation of the neoblasts. Taken together, these  
254 results indicated that the neoblasts were highly enriched but could not undergo differentiation in the  
255 homeostatic condition of *cdhl* KD planarians.

256

257 ***cdhl* was required for the neoblasts to respond to ERK signaling and undergo differentiation**  
258 **during regeneration**

259           While control animals showed a differentiating *piwiA* negative blastema region at 3 dpa, *cdhl*  
260    KD animals did not have *piwiA* negative region (Fig. 4A). This regeneration defect resembled that of  
261    ERK inhibitor-treated animals (Tasaki et al., 2011a). ERK signaling has been thought to be an  
262    induction signal in planarians since an ERK inhibitor (U0126) and the knockdown of *erk-A* inhibited  
263    the differentiation of the neoblasts in both homeostatic and regenerating conditions (Tasaki et al.,  
264    2011a). Therefore, we speculated that the ERK signaling was not activated in the neoblasts in *cdhl*  
265    KD animals and caused the failure of blastema formation. However, surprisingly, western blotting  
266    analysis using antibody against the phosphorylated active form of ERK (pERK) revealed that pERK  
267    was detected near the stump of both control and *cdhl* KD animals at 1 dpa, while U0126 effectively  
268    inhibited the phosphorylation of ERK (Fig. 4B). To check the pERK activity in the neoblasts, we  
269    conducted double WISH of *piwiA* and *mkpA*, a reliable target gene of ERK signaling (Tasaki et al.,  
270    2011a; Umesono et al., 2013). *mkpA* was highly expressed near the stump at 1 dpa in control and *cdhl*  
271    KD animals, and U0126 treatment of control animals inhibited the *mkpA* expression (Fig. 4C). While  
272    most of the *mkpA* expression in control animals was observed in differentiated or differentiating *piwiA*  
273    negative cells, *mkpA* was largely expressed in *piwiA* positive neoblasts in *cdhl* KD animals. These  
274    results indicated that the ERK signaling was definitely activated in the neoblasts even in *cdhl* KD  
275    animals, but differentiation did not occur. To quantify the pERK activity, we conducted RT-qPCR  
276    analysis of *mkpA*. The result showed that the expression of *mkpA* was comparable between control and  
277    *cdhl* KD animals (Fig. 4D). Taken together, these results suggested that the neoblasts in *cdhl* KD  
278    animals could receive almost the same amount of ERK signaling activation, but they could not respond  
279    to the signal, and therefore the neoblasts could not undergo differentiation.

280           Taken altogether, our findings show that the neoblasts in *cdhl* KD animals, which could not  
281    arrest the cell cycle, did not undergo differentiation even though they received an induction signal.  
282    Thus, our results indicate that cell cycle arrest is required by stem cells for the acquisition of

283 competence to differentiate. Alternatively, it could be thought that stem cells persist in their

284 undifferentiated state as long as their cell cycle is progressing.

285

286 **Discussion**

287 In this report, we showed that planarians seem to lack most cell cycle regulator genes, but  
288 possess *cdh1* as their only gene causing cell cycle exit, suggesting that planarians could have a quite  
289 simple cell cycle regulation in which only Cdh1 expression regulated cell cycle exit. The *cdh1* KD  
290 planarians did not maintain tissue homeostasis and also did not regenerate their body after amputation.  
291 Under conditions that induced homeostasis in control planarians, the mitotic neoblasts in *cdh1* KD  
292 planarians, including PSCs, were drastically propagated while the progenitor cells and the  
293 differentiated cells were decreased. Furthermore, the neoblasts in *cdh1* KD animals could not undergo  
294 differentiation to form a blastema although the ERK signaling as an induction signal was definitely  
295 activated. These results indicated that *cdh1* KD enhanced self-renewal of the neoblasts, and the  
296 neoblasts in the proliferative state could not undergo differentiation.

297 Our results summarized above strongly indicated that proliferative stem cells could not respond  
298 to induction signals. In other words, it is possible to think that maintenance of the proliferative state  
299 ensures the undifferentiated state. Interestingly, Tgs1, a candidate marker for PSCs among neoblasts  
300 (Zeng et al., 2018), carries APC/C-Cdh1 target sequences such as a D-box. This indicates that Tgs1  
301 would be degraded, and then cells would lose the identity of PSCs upon the expression of *cdh1*, which  
302 supports a direct association between pluripotency and cell cycling. Further, animal cap cells of  
303 *Xenopus* blastulae are pluripotent, but the pluripotency disappears at the onset of gastrulation,  
304 excluding the prospective neural crest region. This is consistent with the previous report that neural  
305 crest cells retain blastula-stage potential during *Xenopus* early development (Buitrago-Delgado et al.,  
306 2015). Coincidentally, though *Xhairy2* is weakly expressed in the entire animal cap region in blastulae,  
307 the *Xhairy2* expression is restricted only in the prospective neural crest region and becomes higher at  
308 gastrula stage or later (Tsuji et al., 2003). Since *Xhairy2* represses *p27* expression to maintain cells in  
309 a proliferative and undifferentiated state, continuous expression of *Xhairy2* from the blastula through

310 the gastrula stage maintains the cell cycling, and this may ensure the pluripotency (Nagatomo and  
311 Hashimoto, 2007).

312 The incompatibility of proliferation and differentiation has been described in a wide variety of  
313 stem cells and organisms for a long time. In *C. elegans* gonad, germ-line stem cells (GSCs) exist only  
314 adjacent to the distal tip cell (DTC) and undergo differentiation when they are apart from DTC. It is  
315 known that the self-renewal of GSCs in *C. elegans* is maintained by the activation of Notch signaling  
316 by DTC, and that all GSCs undergo differentiation in recessive mutants of GLP-1, a Notch homolog  
317 in *C. elegans* (Austin and Kimble, 1987). Similarly, GSCs in male *Drosophila melanogaster* exist only  
318 when they contact hub cells through E-cadherin. The GSCs that contact hub cells receive Unpaired  
319 and activate JAK-STAT signaling to proliferate, while GSCs not in contact with hub cells cannot  
320 receive a sufficient amount of Unpaired and they therefore undergo differentiation (Kiger et al., 2001;  
321 Tulina and Matunis, 2001). Although different molecular pathways are activated in the GSCs of the  
322 above two invertebrate species, the GSCs share the feature that they exist as stem cells in a  
323 microenvironment promoting self-renewal, and undergo differentiation when self-renewal cannot be  
324 maintained. This raises the possibility that the difference of the activated signaling pathway in stem  
325 cells is due to the difference of how to maintain the stem cells' cell cycle progression. Consistently,  
326 *cyclin D* KD planarians, which are thought to undergo forced cell cycle arrest, could not regenerate  
327 their missing body parts and lost the neoblasts (Fig. S5). These reports and our results indicate that the  
328 cell cycle should be maintained for stem cells to exist in tissues without differentiation.

329 The incompatibility of proliferation and differentiation is also reported in the regulation of  
330 transcription factors and chromatin status. Cyclin D-CDK and cyclin E-CDK complexes  
331 phosphorylate Oct4, Sox2 and Nanog to stabilize these transcription factors from proteasomal  
332 degradation in mouse ESCs, suggesting that cell cycle progression maintains a stem cell state (Liu et  
333 al., 2017). Conversely, the transcriptional activity of MyoD, a master regulator of muscle

334 differentiation whose ectopic expression causes the expression of the muscle-specific genes in many  
335 cell types, is activated only at G1 phase in murine myoblasts (Skapek et al., 1995). The proneuronal  
336 differentiation factor NGN-2 is phosphorylated by Cyclin A- and Cyclin B-CDK complexes and this  
337 phosphorylation impairs the DNA-binding of NGN2 during S through M phase in mice and *Xenopus*  
338 (Ali et al., 2011; Hindley et al., 2012). Moreover, H3K4me3 active histone marks are increased at G1  
339 phase, while H3K27me3 repressive histone marks are stable throughout the cell cycle at  
340 developmentally regulated genes of human ESCs. This suggested that the developmentally regulated  
341 genes become bivalent at only G1 phase, which allows the transcription factors to be loaded (Singh et  
342 al., 2015). Our results also showed that the neoblasts in *cdhl* KD planarians could not undergo  
343 differentiation though they had phosphorylated ERK (Fig. 4). These examples indicate that stem cells  
344 in the proliferative state could not undergo differentiation even if they expressed potent differentiation-  
345 specific transcription factors.

346 In addition, stalk cell differentiation of cellular slime mold *Dictyostelium* requires cell cycle  
347 arrest. This suggests that the incompatibility between proliferation and differentiation is a universal  
348 trait of cells beyond the animal kingdom. Interestingly, DIF-1, an inducer of stalk cell differentiation  
349 in *Dictyostelium*, suppresses the expression of *cyclin D* and *cyclin E* and induces the differentiation of  
350 mouse vascular smooth muscle cells and the re-differentiation of mouse leukemia cells (Miwa et al.,  
351 2000; Asahi et al., 1995). Furthermore, we observed upregulation of *mkpA* in planarians treated with  
352 DIF-1. It could be thought that DIF-1 also induced the activation of ERK as induction signal in  
353 planarians (Fig. S6A). However, DIF-1 treatment of *cdhl* KD planarians did not cause blastema  
354 formation, which confirmed that stem cells with cell cycle progression could not undergo  
355 differentiation even though the induction signal was artificially activated (Fig. S6B).

356 Taking these facts all together, we propose that stem cells may persist in their undifferentiated  
357 state as long as their cell cycle is progressing, and cell cycle arrest might dictate that stem cells become



358 competent to differentiate according to their surroundings. Although the activated signaling pathways  
359 and transcription factors vary among stem cells, it could be thought that the incompatibility of  
360 proliferation and differentiation is a universal feature conserved from *Dictyostelium* to mammals.

361

362 It has been reported that differentiation occurs at G1 phase in various stem cells and that  
363 differentiation is induced by functional inhibition of Cyclins or CDKs (Lange and Calegari, 2010).  
364 These reports make us speculate that stem cells stochastically undergo differentiation depending on  
365 whether their cell cycle phase is G1 or not. The differentiation at G1 phase could possibly explain the  
366 stochastic differentiation model which has been proposed for ESCs and a range of adult tissue  
367 homeostasis (Stumpf et al., 2017, Simons and Clevers, 2011). If this speculation is correct, the  
368 proliferating neoblasts in *cdh1* KD animals also stochastically undergo differentiation during G1 phase  
369 in the ongoing cell cycle. However, the differentiated cells and the progenitor cells were definitely  
370 decreased in *cdh1* KD animals, which caused disruption of tissue homeostasis and regeneration. Since  
371 *cdh1* is known to play an important role in cell cycle arrest, it could be suggested that differentiation  
372 occurs when the cell cycle is arrested but not during the progressing G1 phase.

373 As mentioned above, *Xhairy2* maintains the proliferative and undifferentiated state by  
374 repressing *p27* during neural crest specification and also in the lens placode of *Xenopus* embryo  
375 (Nagatomo and Hashimoto, 2007; Murato and Hashimoto, 2009). However, the prospective neural  
376 crest region or lens placode did not show frequent cell division compared to the other regions of the  
377 embryo. Thus, it could be thought that these cells do not completely stop the cell cycle but just pause  
378 at G1 phase. Reversible growth arrest has been described just as “quiescence” so far, but here we  
379 would like to propose two substantially different quiescent states, namely, G1 arrest and G0: cells in  
380 G1 arrest might be just transiently paused but still remain in G1 phase to persist in their  
381 undifferentiated state, but cells in G0 phase might completely stop proliferation and exit the cell cycle

382 for the acquisition of competence. Although we could not distinguish between G1 arrest and G0 yet,  
383 we expect that further research on the cell cycle and differentiation competence will delineate the  
384 difference underlying the two quiescent states.

385

386 During the development of most multicellular organisms, stepwise differentiation occurs in  
387 parallel at various time points and regions. According to our model described above, cells must exit  
388 the cell cycle in order to undergo differentiation, and re-enter the cell cycle to increase the cell number.  
389 This combination of steps of proliferation and differentiation may correspond to the seeming stepwise  
390 differentiation. Furthermore, multiple mechanisms regulating cell cycle exit should be required for  
391 parallel and spatiotemporal differentiation. Such a requirement for complicated cell cycle regulation  
392 could possibly explain why most multicellular organisms conserve numerous factors involved in cell  
393 cycle regulation. However, it was suggested that planarians have a quite simple cell cycle regulation  
394 which lacks most of the cell cycle regulators such as CKIs. The differentiated cells in planarians are  
395 supplied directly from the neoblasts and never proliferate, which might allow the simplification of cell  
396 cycle regulation. In addition, cell cycle regulation without CKI expression is also observed in mouse  
397 ESCs. Due to the absence of CKI expression, CDK activity is constitutively high in mouse ESCs, and  
398 their G1 phase is quite short (about 3 hours) compared to that of mouse embryonic fibroblasts (11  
399 hours; Liu et al., 2019). Therefore, it is conceivable that planarians could have lost CKI genes which  
400 are dispensable for cell cycle regulation of PSCs. In other words, planarian cell cycle regulation might  
401 not be species-specifically anomalous, but instead might be regulation common among PSCs. Studies  
402 of planarians, which have simplified cell cycle regulation, will reveal the nature of features of  
403 proliferation and differentiation conserved among multicellular organisms.

404 The remarkable regenerative ability of planarians has fascinated many researchers, and the  
405 availability of methods for functional inhibition by RNAi in planarians provides a great opportunity

406 to study gene function in planarians. However, the lack of a means for gain-of-function in planarians  
407 still makes these studies difficult. For this purpose, effective isolation and amplification of PSCs is  
408 needed. In this report, we showed the drastic enrichment of the neoblasts throughout the body of *cdhl*  
409 KD animals, which could be regarded as “culture flasks of the neoblasts”. Therefore, the functional  
410 inhibition of *cdhl* may enable us to establish not only the gain-of-function but also gene knockout,  
411 conditional mutagenesis and other genetic manipulations, which could be a key to the next step of  
412 planarian research.

413

#### 414 **Acknowledgements**

415 We thank Dr. Kazuyuki Fujimitsu for helpful discussions, Miyuki Ishida for technical  
416 assistance and critical discussions, and Dr. Elizabeth Nakajima for critical reading of the manuscript.

417

#### 418 **Author contributions**

419 Conceptualization: Y.U., C.H.; Methodology: Y.S., Y.K.; Validation: Y.S.; Formal analysis: Y.S.,  
420 Y.K.; Investigation: Y.S.; Resources: K.A., C.H.; Writing-original draft preparation: Y.S., C.H.;  
421 Supervision: C.H.; Project administration: Y.U., C.H.; Funding acquisition: C.H.

422

423 **Materials and methods**

424 **Animals**

425 The clonal SSP-9T strain of the planarian *Dugesia japonica* (Nishimura et al., 2015), derived from  
426 the Iruma River in Gifu prefecture, Japan, was maintained in dechlorinated tap water at 21°C, which  
427 is a suitable condition for maintaining the population size (Mori et al, 2019). Chicken liver was fed  
428 to them one or two times a week. Planarians ~6 mm in length were starved for at least 1 week before  
429 experiments. The animal experimentation was conducted according to the protocol reviewed and  
430 approved by the Institutional Animal Care and Use Committee of JT Biohistory Research Hall.

431

432 **Molecular cloning of planarian *cdh1* gene**

433 The transcriptome dataset of *D. japonica* (Shibata et al., 2016) was used for gene identification, and  
434 we thereby found the planarian *cdh1* gene (accession number: IAAB01050803). cDNA of the gene  
435 was obtained by PCR using a set of primers (Fw: 5'-  
436 ATGGATAGTTCATATGAACGTCGATTATT-3' and Rv: 5'-  
437 TTATCTCATAACCACTGAACAAATCGAGAGC-3'), and cloned into pCS2 vector and  
438 sequenced.

439

440 **Inhibitor treatment**

441 The JNK inhibitor SP600125 (Sigma-Aldrich) and the MAPK/ERK (MEK) inhibitor U0126 (Cell  
442 Signaling Technology) were dissolved in dimethylsulfoxide (DMSO) as 25 mM. DIF-1 (Sigma-  
443 Aldrich) was dissolved in DMSO at 500 µM. Planarians were kept in dechlorinated tap water  
444 containing 0.1% DMSO, 25 µM SP600125, 25 µM U0126 or 500 nM DIF-1 with light shielding.  
445 The inhibitor-containing breeding water was replaced with fresh inhibitor-containing breeding water  
446 every day.

447

448 **Whole-mount in situ hybridization**

449 Planarians were treated with 2% hydrochloric acid in 5/8 Holtfreter's solution for 5 minutes at room  
450 temperature to remove mucus and fixed with 4% paraformaldehyde, 5% methanol in 11/14 PBS for  
451 30 minutes at room temperature. Hybridization and staining of digoxigenin (DIG)- or fluorescein  
452 (FITC)- labelled probes were conducted as described previously (Umesono et al., 1997). After the  
453 hybridization, samples were washed and treated with 1% blocking reagent (Roche). For alkaline  
454 phosphatase staining, samples were incubated with anti-DIG-AP antibody (Roche, 11093274910)  
455 overnight, and color development was conducted with BCIP/NBT substrate (Roche). For fluorescent  
456 staining, anti-DIG-POD (Roche, 11207733910) or anti-FITC-POD (Roche, 11772465001) antibody  
457 was used for overnight incubation. To optimize the fluorescent staining, we washed samples with  
458 borate buffer (100 mM borate (pH 8.5), 0.1% Tween-20), and conducted tyramide signal  
459 amplification in TSA reaction solution (a tyramide reagent, 0.003% H<sub>2</sub>O<sub>2</sub>, 2% dextran sulfate  
460 sodium salt and 0.3 mg/mL 4-iodo-phenol in borate buffer) according to Lauter et al., 2011 and  
461 Akiyama-Oda and Oda, 2016.

462

463 **Whole-mount immunostaining of pH3**

464 Samples were fixed and immunostaining was conducted according to a previous report (Tasaki  
465 et al., 2011a). Anti-pH3 antibody (Sigma-Aldrich, 06-570) was used at 1/200 dilution as first  
466 antibody, and anti-rabbit IgG-Alexa 488 (Invitrogen, A11034) was used at 1/1,000 dilution as  
467 secondary antibody.

468

469 **Section in situ hybridization**

470 Planarians were treated with 2% hydrochloric acid in 5/8 Holtfreter's solution for 5 minutes at room

471 temperature to remove mucus and fixed with relaxant solution (1% nitric acid/ 1.6% formaldehyde/  
472 0.02 mM MgSO<sub>4</sub>) overnight at 4°C. The following procedures were conducted as previously  
473 described (Kobayashi et al., 1998).

474

#### 475 **Feeding RNAi**

476 Double-stranded RNA (dsRNA) was synthesized based on a previous report (Rouhana et al., 2013).  
477 A DNA fragment containing the target gene sequence with the T7 promoter at both ends was used as  
478 the template for dsRNA synthesis. The synthesis was conducted with a Megascript T7 transcription  
479 kit (Thermo Fisher Scientific) following the manufacturer's protocol. The synthesized dsRNA was  
480 treated with TURBO DNase and RNase T1 (Roche) for 1 h at 37°C to remove DNA template and  
481 single-stranded RNA. The dsRNA was precipitated with LiCl and dissolved in water at 250 ng/μL.  
482 Thirty planarians were fed a mixture of 25 μL of 50% chicken liver homogenate (w/v), 5 μL of 2%  
483 agarose (w/v), and 10 μL of dsRNA solution, once daily for 3 h. The mixture was divided into small  
484 aliquots and frozen at -30°C before feeding. The feeding was conducted on four successive days and  
485 on the day of 1 week after the first feeding. Control animals were fed dsRNA of *enhanced green*  
486 *fluorescent protein (EGFP)*.

487

#### 488 **RT-qPCR analysis**

489 Total RNA was extracted from 3-5 planarians by using ISOGEN-LS (Wako) following the  
490 manufacturer's protocol. cDNA was synthesized from 1 μg total RNA using a PrimeScript RT reagent  
491 kit (Takara) according to the manufacturer's instructions. The synthesized cDNA was diluted 1:20,  
492 and qPCR reactions were conducted in 20 μL of a mixture containing 1x TB Green premix Ex TaqII  
493 (Takara), 0.3 μM gene-specific forward/reverse primers and 2 μL of diluted cDNA using a thermal  
494 cycler Dice (Takara). The reactions were carried out as follows: 95°C for 30 sec, 40 cycles of 95°C

495 for 15 s, 60°C for 30 s, 72°C for 1 min. The expression of each gene was normalized by the expression  
496 of *g3pdh*. All experiments were performed using three biological and three technical replicates. The  
497 sequences of gene-specific primers are listed in table S1.

498

#### 499 **FACS analysis**

500 Cell dissociation was performed from ten planarians as previously described (Hayashi et al., 2006).  
501 The number of dissociated cells was counted using a LUNA-FL (Logos Biosystems). The dissociated  
502 cells were stained with 18 µg/mL Hoechst 33342 and 0.1 µg/mL Calcein AM for 2 h at 20°C. FACS  
503 analysis was conducted using blue and violet lasers of BD FACSMelody (BD Bioscience) and FlowJo  
504 (v10.7.1, BD Bioscience) (Kuroki, unpublished). Experiments were performed using three biological  
505 replicates.

506

#### 507 **EdU labeling and detection**

508 Thirty planarians were fed a mixture of 20 µL of 50% chicken liver homogenate (w/v), 5 µL of 2%  
509 agarose (w/v), 10 µL of the indicated dsRNA solution and 14 µL of 20 mg/mL EdU for 3 h. The  
510 mixture had been divided into small aliquots and frozen at -30°C before feeding. The animals were  
511 fixed and subjected to whole-mount in situ hybridization as described above. After that, EdU detection  
512 was conducted using a Click-iT EdU imaging kit (Invitrogen) according to the manufacturer's protocol.

513

#### 514 **Western blotting**

515 Blastemas were dissected from 20 regenerating planarians at 1 dpa, pooled, and dissolved in 50 µl of  
516 sample buffer (0.01 M Tris-HCl, 2% SDS, 6% 2-mercaptethanol, 10% glycerol) and were sonicated  
517 and boiled for 5 minutes. 5 µl of the samples was subjected to SDS-PAGE and western blotting.  
518 Membrane blocking was conducted by using Blocking Reagent (Roche). The primary antibodies were

519 rabbit anti-phosphorylated ERK (1/500; Tasaki et al., 2011a) or mouse anti- $\alpha$ -tubulin monoclonal  
520 antibody DM 1A (1/5,000; Sigma-Aldrich, T9026). An appropriate antibody conjugated with  
521 horseradish peroxidase (1/5,000) was used as secondary antibody. ImmunoStar Zeta (Wako) was used  
522 for signal detection.

523

#### 524 **Phylogenetic analysis**

525 The amino acid sequences of Cdh1 from various organisms and CDC20 from *Drosophila*  
526 *melanogaster* were aligned using the ClustalW program. A phylogenetic tree was reconstructed from  
527 the alignment by the neighbor joining method with the JTT model included in Mega X software.

528

#### 529 **Statistical analysis**

530 Statistical analyses were performed using Microsoft Excel. Two-sided Student's *t*-tests ( $\alpha = 0.05$ )  
531 were performed to compare the means of two populations.

532

533



534 **References**

- 535 1. Agata K, Watanabe K. (1999). Molecular and cellular aspects of planarian regeneration. *Semin*  
536 *Cell Dev Biol.* **10**, 377-383.
- 537 2. Akiyama-Oda Y, Oda H. (2016). Multi-color FISH facilitates analysis of cell-type diversification  
538 and developmental gene regulation in the *Parasteatoda* spider embryo. *Dev Growth Differ.* **58**,  
539 215-224.
- 540 3. Ali F, Hindley C, McDowell G, Deibler R, Jones A, Kirschner M, Guillemot F, Philpott A.  
541 (2011). Cell cycle-regulated multi-site phosphorylation of Neurogenin 2 coordinates cell cycling  
542 with differentiation during neurogenesis. *Development.* **138**, 4267-4277.
- 543 4. An Y, Kawaguchi A, Zhao C, Toyoda A, Sharifi-Zarchi A, Mousavi SA, Bagherzadeh R, Inoue T,  
544 Ogino H, Fujiyama A, Chitsaz H, Baharvand H, Agata K. (2018). Draft genome of *Dugesia*  
545 *japonica* provides insights into conserved regulatory elements of the brain restriction gene *nou-*  
546 *darake* in planarians. *Zoological Lett.* **4**, 24.
- 547 5. Asahi K, Sakurai A, Takahashi N, Kubohara Y, Okamoto K, Tanaka Y. (1995). DIF-1, morphogen  
548 of *Dictyostelium discoideum*, induces the erythroid differentiation in murine and human leukemia  
549 cells. *Biochem Biophys Res Commun.* **208**, 1036-1039.
- 550 6. Austin J, Kimble J. (1987). *glp-1* is required in the germ line for regulation of the decision between  
551 mitosis and meiosis in *C. elegans*. *Cell.* **51**, 589-599.
- 552 7. Avraham R, Yarden Y. (2011). Feedback regulation of EGFR signalling: decision making by early  
553 and delayed loops. *Nat Rev Mol Cell Biol.* **12**, 104-117.
- 554 8. Buitrago-Delgado E, Nordin K, Rao A, Geary L, LaBonne C. (2015). Shared regulatory programs  
555 suggest retention of blastula-stage potential in neural crest cells. *Science.* **348**:1332-1335.
- 556 9. Cappell SD, Chung M, Jaimovich A, Spencer SL, Meyer T. (2016). Irreversible APC(Cdh1)  
557 Inactivation Underlies the Point of No Return for Cell-Cycle Entry. *Cell.* **166**, 167-180.

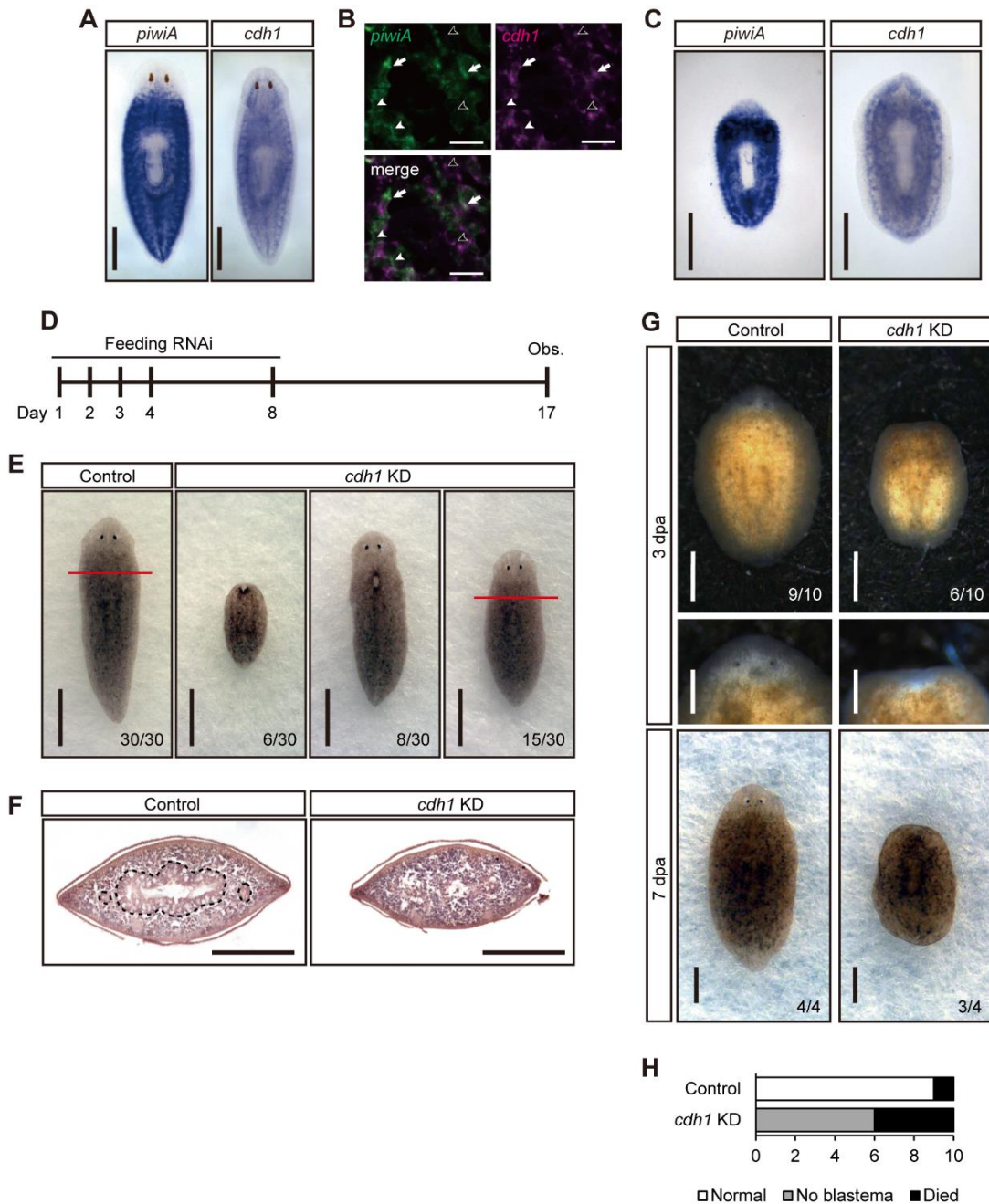
- 558 10. Grohme MA, Schloissnig S, Rozanski A, Pippel M, Young GR, Winkler S, Brandl H, Henry I,  
559 Dahl A, Powell S, Hiller M, Myers E, Rink JC. (2018). The genome of *Schmidtea mediterranea*  
560 and the evolution of core cellular mechanisms. *Nature*. **554**, 56-61.
- 561 11. Hayashi T, Asami M, Higuchi S, Shibata N, Agata K. (2006). Isolation of planarian X-ray-  
562 sensitive stem cells by fluorescence-activated cell sorting. *Dev Growth Differ*. **48**, 371-380.
- 563 12. Hayashi T, Shibata N, Okumura R, Kudome T, Nishimura O, Tarui H, Agata K. (2010). Single-  
564 cell gene profiling of planarian stem cells using fluorescent activated cell sorting and its "index  
565 sorting" function for stem cell research. *Dev Growth Differ*. **52**, 131-144.
- 566 13. Hindley C, Ali F, McDowell G, Cheng K, Jones A, Guillemot F, Philpott A. (2012). Post-  
567 translational modification of Ngn2 differentially affects transcription of distinct targets to regulate  
568 the balance between progenitor maintenance and differentiation. *Development*. **139**, 1718-1723.
- 569 14. Kiger AA, Jones DL, Schulz C, Rogers MB, Fuller MT. (2001). Stem cell self-renewal specified  
570 by JAK-STAT activation in response to a support cell cue. *Science*. **294**, 2542-2545.
- 571 15. Kobayashi, C., Kobayashi, S., Orii, H., Watanabe, K. & Agata, K. (1998). Identification of two  
572 distinct muscles in the planarian *Dugesia japonica* by their expression of myosin heavy chain  
573 genes. *Zoolog. Sci*. **15**, 861–869.
- 574 16. Kunath T, Saba-El-Leil MK, Almousaillekh M, Wray J, Meloche S, Smith A. (2007). FGF  
575 stimulation of the Erk1/2 signalling cascade triggers transition of pluripotent embryonic stem cells  
576 from self-renewal to lineage commitment. *Development*. **134**, 2895-2902.
- 577 17. Lange C, Calegari F. (2010). Cdks and cyclins link G1 length and differentiation of embryonic,  
578 neural and hematopoietic stem cells. *Cell Cycle*. **9**, 1893-1900.
- 579 18. Lauter G, Söll I, Hauptmann G. (2011). Multicolor fluorescent in situ hybridization to define  
580 abutting and overlapping gene expression in the embryonic zebrafish brain. *Neural Dev*. **6**, 10.
- 581 19. Liu L, Michowski W, Inuzuka H, Shimizu K, Nihira NT, Chick JM, Li N, Geng Y, Meng AY,

- 582 Ordureau A, Kołodziejczyk A, Ligon KL, Bronson RT, Polyak K, Harper JW, Gygi SP, Wei W,  
583 Sicinski P. (2017). G1 cyclins link proliferation, pluripotency and differentiation of embryonic  
584 stem cells. *Nat Cell Biol.* **19**, 177-188.
- 585 20. Liu L, Michowski W, Kolodziejczyk A, Sicinski P. (2019). The cell cycle in stem cell proliferation,  
586 pluripotency and differentiation. *Nat Cell Biol.* **21**, 1060-1067.
- 587 21. Marshall CJ. (1995). Specificity of receptor tyrosine kinase signaling: transient versus sustained  
588 extracellular signal-regulated kinase activation. *Cell.* **80**, 179-185.
- 589 22. Miwa Y, Sasaguri T, Kosaka C, Taba Y, Ishida A, Abumiya T, Kubohara Y. (2000). Differentiation-  
590 inducing factor-1, a morphogen of *dictyostelium*, induces G(1) arrest and differentiation of  
591 vascular smooth muscle cells. *Circ Res.* **86**, 68-75.
- 592 23. Mori M, Narahashi M, Hayashi T, Ishida M, Kumagai N, Sato Y, Bagherzadeh R, Agata K, Inoue  
593 T. (2019). Calcium ions in the aquatic environment drive planarians to food. *Zoological Lett.* **5**,  
594 31.
- 595 24. Murato Y, Hashimoto C. (2009). Xhairy2 functions in *Xenopus* lens development by regulating  
596 p27(xic1) expression. *Dev Dyn.* **238**, 2179-2192.
- 597 25. Nadal-Ginard B. (1978). Commitment, fusion and biochemical differentiation of a myogenic cell  
598 line in the absence of DNA synthesis. *Cell.* **15**, 855-864.
- 599 26. Nagatomo K, Hashimoto C. (2007). *Xenopus hairy2* functions in neural crest formation by  
600 maintaining cells in a mitotic and undifferentiated state. *Dev Dyn.* **236**, 1475-1483.
- 601 27. Newmark PA, Sánchez Alvarado A. (2000). Bromodeoxyuridine specifically labels the  
602 regenerative stem cells of planarians. *Dev Biol.* **220**, 142-153.
- 603 28. Newmark PA, Sánchez Alvarado A. (2002). Not your father's planarian: a classic model enters the  
604 era of functional genomics. *Nat Rev Genet.* **3**, 210-219.
- 605 29. Nishimura O, Hosoda K, Kawaguchi E, Yazawa S, Hayashi T, Inoue T, Umesono Y, Agata K.

- 606 (2015). Unusually Large Number of Mutations in Asexually Reproducing Clonal Planarian  
607 *Dugesia japonica*. *PLoS One*. **10**, e0143525.
- 608 30. Pauklin S, Vallier L. (2013). The cell-cycle state of stem cells determines cell fate propensity. *Cell*.  
609 **155**, 135-147.
- 610 31. Pearson BJ, Sánchez Alvarado A. (2010). A planarian p53 homolog regulates proliferation and  
611 self-renewal in adult stem cell lineages. *Development*. **137**, 213-221.
- 612 32. Roberts-Galbraith RH, Newmark PA. (2015). On the organ trail: insights into organ regeneration  
613 in the planarian. *Curr Opin Genet Dev*. **32**, 37-46.
- 614 33. Rouhana L, Weiss JA, Forsthoefel DJ, Lee H, King RS, Inoue T, Shibata N, Agata K, Newmark  
615 PA. (2013). RNA interference by feeding in vitro-synthesized double-stranded RNA to planarians:  
616 methodology and dynamics. *Dev Dyn*. **242**, 718-730.
- 617 34. Sasai Y, De Robertis EM. (1997). Ectodermal patterning in vertebrate embryos. *Dev Biol*. **182**, 5-  
618 20.
- 619 35. Simons BD, Clevers H. (2011). Strategies for homeostatic stem cell self-renewal in adult tissues.  
620 *Cell*. **145**, 851-862.
- 621 36. Singh AM, Sun Y, Li L, Zhang W, Wu T, Zhao S, Qin Z, Dalton S. (2015). Cell-Cycle Control of  
622 Bivalent Epigenetic Domains Regulates the Exit from Pluripotency. *Stem Cell Reports*. **5**, 323-  
623 336.
- 624 37. Shibata N, Rouhana L, Agata K. (2010). Cellular and molecular dissection of pluripotent adult  
625 somatic stem cells in planarians. *Dev Growth Differ*. **52**, 27-41.
- 626 38. Shibata N, Kashima M, Ishiko T, Nishimura O, Rouhana L, Misaki K, Yonemura S, Saito K, Siomi  
627 H, Siomi MC, Agata K. (2016). Inheritance of a Nuclear PIWI from Pluripotent Stem Cells by  
628 Somatic Descendants Ensures Differentiation by Silencing Transposons in Planarian. *Dev Cell*.  
629 **37**, 226-237.

- 630 39. Skapek SX, Rhee J, Spicer DB, Lassar AB. (1995). Inhibition of myogenic differentiation in  
631 proliferating myoblasts by cyclin D1-dependent kinase. *Science*. **267**, 1022-1024.
- 632 40. Stavridis MP, Lunn JS, Collins BJ, Storey KG. (2007). A discrete period of FGF-induced Erk1/2  
633 signalling is required for vertebrate neural specification. *Development*. **134**, 2889-2894.
- 634 41. Stumpf PS, Smith RCG, Lenz M, Schuppert A, Müller FJ, Babbie A, Chan TE, Stumpf MPH,  
635 Please CP, Howison SD, Arai F, MacArthur BD. (2017). Stem Cell Differentiation as a Non-  
636 Markov Stochastic Process. *Cell Syst*. **5**, 268-282.e7.
- 637 42. Tasaki J, Shibata N, Nishimura O, Itomi K, Tabata Y, Son F, Suzuki N, Araki R, Abe M, Agata K,  
638 Umesono Y. (2011a). ERK signaling controls blastema cell differentiation during planarian  
639 regeneration. *Development*. **138**, 2417-2427.
- 640 43. Tasaki J, Shibata N, Sakurai T, Agata K, Umesono Y. (2011b). Role of c-Jun N-terminal kinase  
641 activation in blastema formation during planarian regeneration. *Dev Growth Differ*. **53**, 389-400.
- 642 44. Tsuji S, Cho KW, Hashimoto C. (2003). Expression pattern of a basic helix-loop-helix  
643 transcription factor *Xhair2b* during *Xenopus laevis* development. *Dev Genes Evol*. **213**, 407-411.
- 644 45. Tulina N, Matunis E. (2001). Control of stem cell self-renewal in *Drosophila* spermatogenesis by  
645 JAK-STAT signaling. *Science*. **294**, 2546-2549.
- 646 46. Umesono Y, Watanabe K, Agata K. (1997). A planarian *orthopedia* homolog is specifically  
647 expressed in the branch region of both the mature and regenerating brain. *Dev Growth Differ*. **39**,  
648 723-727.
- 649 47. Umesono Y, Tasaki J, Nishimura Y, Hrouda M, Kawaguchi E, Yazawa S, Nishimura O, Hosoda  
650 K, Inoue T, Agata K. (2013). The molecular logic for planarian regeneration along the anterior-  
651 posterior axis. *Nature*. **500**, 73-76.
- 652 48. Wells RS. (1982). An in vitro assay for growth regulation of embryonal carcinoma by the  
653 blastocyst. *Cancer Res*. **42**, 2736-2741.

- 654 49. Yoshida-Kashikawa M, Shibata N, Takechi K, Agata K. (2007). DjCBC-1, a conserved DEAD  
655 box RNA helicase of the RCK/p54/Me31B family, is a component of RNA-protein complexes in  
656 planarian stem cells and neurons. *Dev Dyn.* **236**, 3436-3450.
- 657 50. Zeng A, Li H, Guo L, Gao X, McKinney S, Wang Y, Yu Z, Park J, Semerad C, Ross E, Cheng  
658 LC, Davies E, Lei K, Wang W, Perera A, Hall K, Peak A, Box A, Sánchez Alvarado A. (2018).  
659 Prospectively Isolated Tetraspanin+ Neoblasts Are Adult Pluripotent Stem Cells Underlying  
660 Planaria Regeneration. *Cell.* **173**, 1593-1608.e20.



661

662 **Fig. 1 The expression pattern of *cdh1* and the phenotype of *cdh1* KD animals.**

663 (A) Expression pattern of *piwiA* and *cdh1* in intact planarian detected by whole-mount in situ

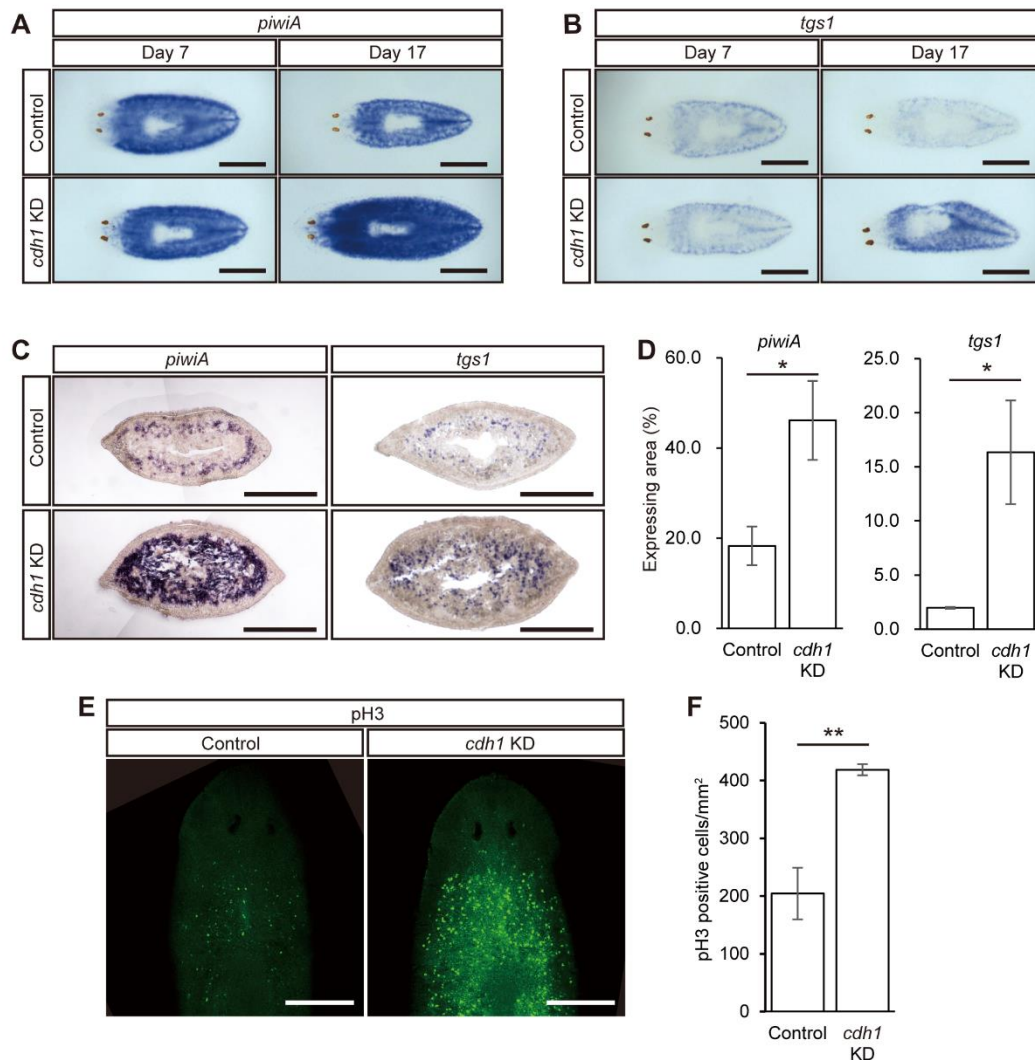
664 hybridization. Cells expressing *cdh1* were observed at periphery of brain and mesenchymal space

665 throughout the body. Scale bars, 1 mm. (B) Double fluorescent in situ hybridization of *piwiA* and

666 *cdh1* in intact animals. Scale bars, 10  $\mu$ m. White arrows indicate *piwiA/cdh1* double positive cells.

667 White arrowheads indicate *piwiA* single positive cells. Black arrowheads indicate *cdhl* single  
668 positive cells. Scale bars, 25  $\mu\text{m}$ . (C) Expression pattern of *piwiA* and *cdhl* at 3 dpa. *cdhl* expression  
669 was also detected in differentiating blastema region. Scale bars, 500  $\mu\text{m}$ . (D) The schedule of  
670 feeding RNAi. The planarians were fed at day 1, 2, 3, 4 and 8. The phenotypes were observed at day  
671 17. (E) The phenotypes of control and *cdhl* KD animals in tissue homeostasis. Whereas all control  
672 animals showed normal morphology, *cdhl* KD animals showed epithelium disorder or headless  
673 phenotype. Red lines indicate the section plane observed in Fig. 1F. Scale bars, 1 mm. (F) HE  
674 staining of transverse section anterior to the pharynx in control and *cdhl* KD animals. Dashed line  
675 indicates the morphology of intestine. The intestinal structure was collapsed in *cdhl* KD animals.  
676 Scale bars, 250  $\mu\text{m}$ . (G) The phenotypes of control and *cdhl* KD animals undergoing regeneration at  
677 3 dpa and 7 dpa. Control animals formed blastema at 3 dpa, and completely regenerated their lost  
678 tissues at 7 dpa. However, *cdhl* KD animals could not form blastema at 3 dpa, and failed to  
679 regenerate at 7 dpa. Scale bars, 500  $\mu\text{m}$  in whole body samples. Scale bars, 250  $\mu\text{m}$  in magnified  
680 view of regenerating head. (H) The number of individuals classified as each phenotype at 3 dpa.  
681





682

683 **Fig. 2 Functional inhibition of *cdh1* caused drastic increase of the neoblasts.**

684 (A) The expression pattern of *piwiA* in intact control animals and *cdh1* KD

685 animals showed more intense expression than control throughout the body at day 17. Scale bar, 500

686  $\mu\text{m}$ . (B) The expression pattern of *tgs1* in intact control animals and *cdh1* KD animals. Like *piwiA*,

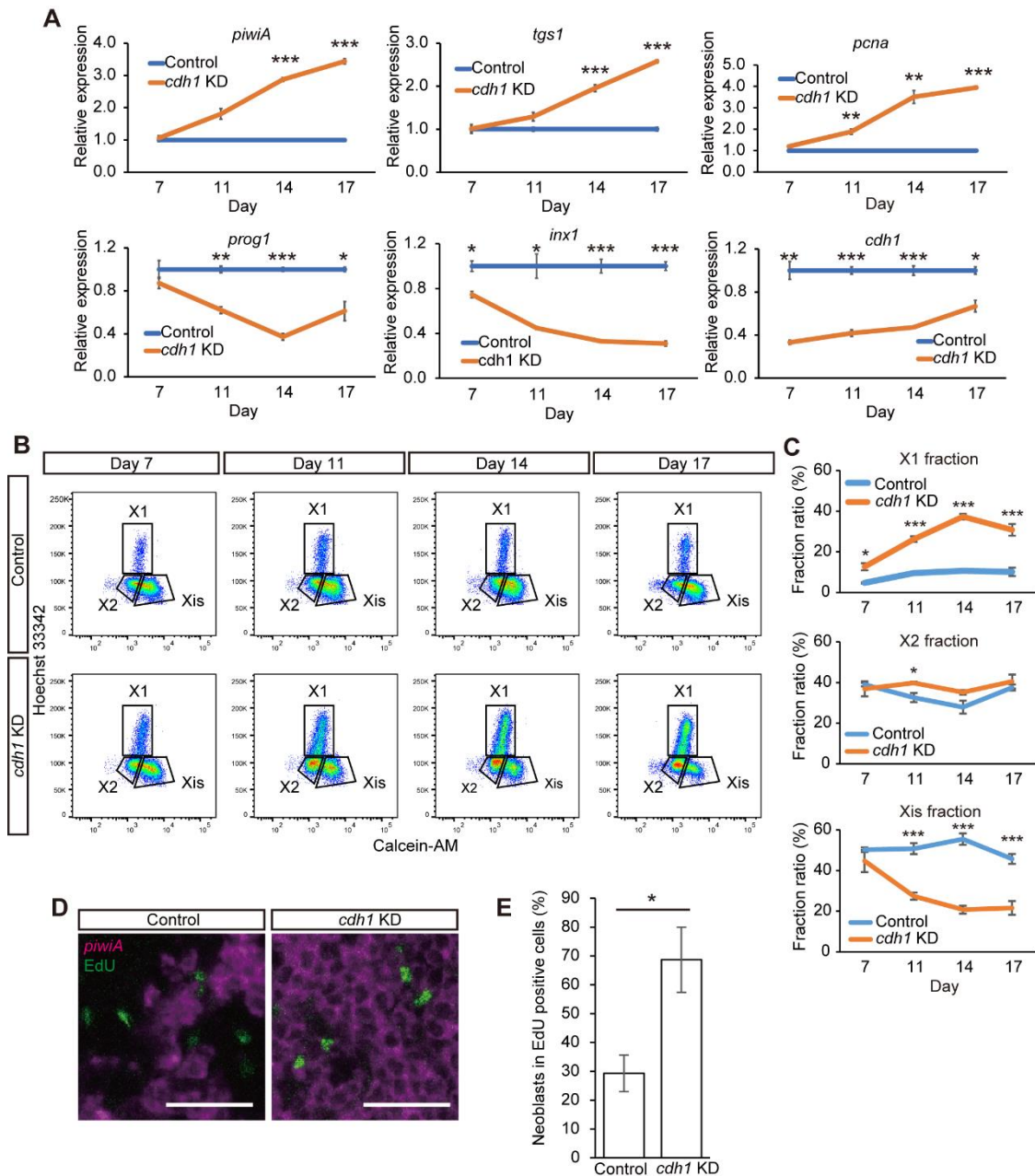
687 *tgs1* was highly expressed in *cdh1* KD animals at day 17. Scale bar, 500  $\mu\text{m}$ . (C) The expression

688 pattern of *piwiA* and *tgs1* in transverse section anterior to the pharynx of control and *cdh1* KD

689 animals at day 17. *piwiA*- and *tgs1*-expressing cells occupied a large area in *cdh1* KD animals. Scale

690 bars, 250  $\mu\text{m}$ . (D) Comparison of the *piwiA*- or *tgs1*-expressing area relative to total mesenchymal

691 area in transverse section anterior to the pharynx of control and *cdhl* KD animals. Data are mean  $\pm$   
692 SEM ( $n = 3$ , Student's *t*-test,  $*p < 0.05$ ). (E) Immunostaining of pH3 in control and *cdhl* KD  
693 planarians. *cdhl* KD animals showed an increased number of pH3-positive cells. Scale bars, 250  
694  $\mu\text{m}$ . (F) The number of pH3-positive cells in control and *cdhl* KD animals. Data are mean  $\pm$  SEM ( $n$   
695 = 3, Student's *t*-test,  $**p < 0.005$ ).  
696

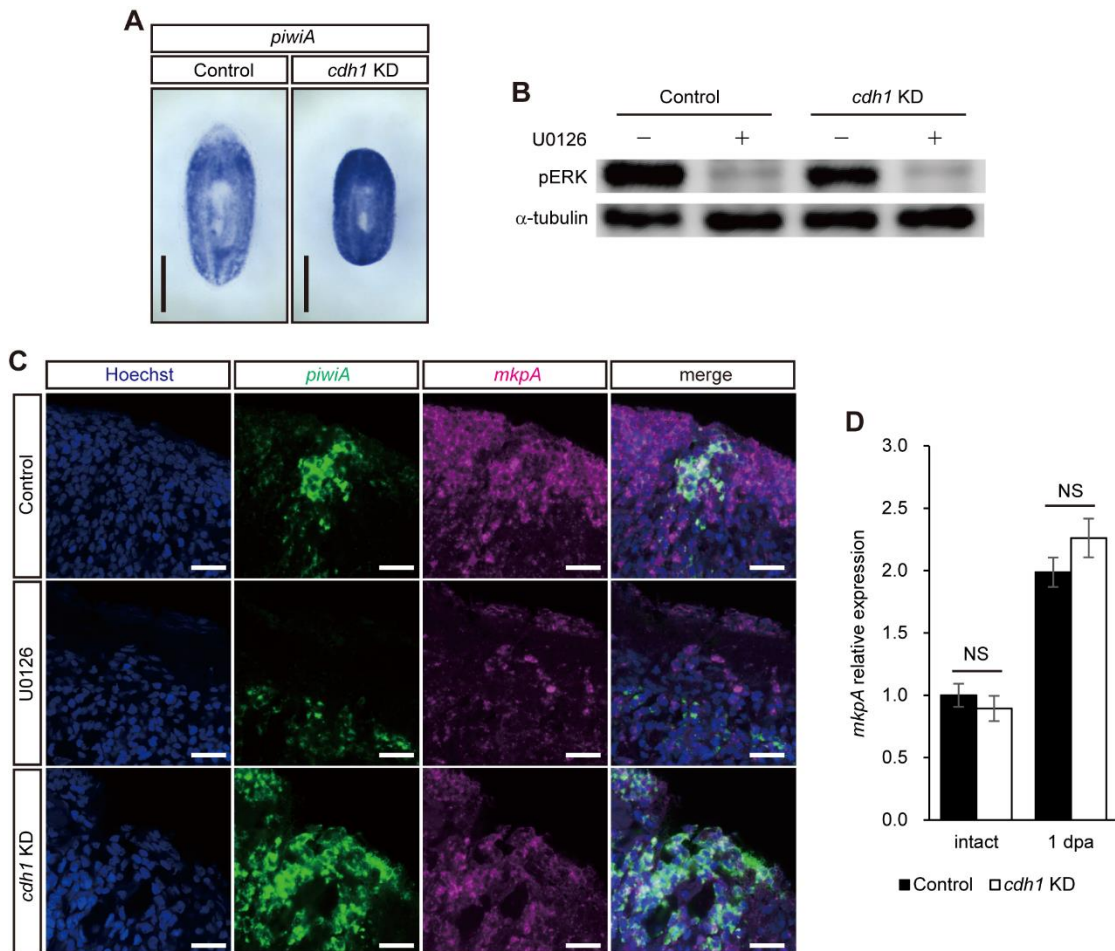


697

698 **Fig. 3 Functional inhibition of *cdh1* suppressed the differentiation of the neoblasts.**

699 (A) The gene expression levels in control and *cdh1* KD animals at day 7, 11, 14 and 17 determined  
 700 by RT-qPCR analysis. The values were relative to in control animals. *cdh1* KD animals showed high  
 701 expression of neoblast marker genes (*piwiA*, *tgs1* and *pcna*) but low expression of a progenitor gene  
 702 (*prog1*) and a differentiated cell gene (*inx1*). Data are mean  $\pm$  SEM (Student's *t*-test, \*  $p < 0.05$ , \*\* $p$

703 < 0.005, \*\*\* $p < 0.001$ ). (B) Representative FACS profiles of cells derived from control and *cdhl*  
704 KD animals at day 7, 11, 14 and 17. The X-axis represents relative intensity of Calcein AM, which  
705 stains cytoplasm. The Y-axis represents relative intensity of Hoechst 33342, which stains nuclei.  
706 Cells that showed low intensity of Calcein AM and high intensity of Hoechst 33342 were designated  
707 the X1 fraction containing the neoblasts at S, G2 and M phase. The X2 fraction showing low  
708 intensity of Calcein AM and low intensity of Hoechst 33342 contains the neoblasts at G1 phase and  
709 a part of differentiated cells. Xis fraction showing high intensity of Calcein AM and low intensity of  
710 Hoechst 33342 contains only differentiated cells. *cdhl* KD animals showed an increase of X1  
711 fraction and a decrease of Xis fraction. (C) Ratio of fraction of X1, X2 and Xis in control and *cdhl*  
712 KD animals. Data are mean  $\pm$  SEM (Student's *t*-test, \*  $p < 0.05$ , \*\*\* $p < 0.001$ ). (D) Fluorescent  
713 staining of *piwiA* and EdU at 3 days after EdU labeling in control and *cdhl* KD animals. Scale bar,  
714 25  $\mu$ m. (E) The percentage of *piwiA*-positive neoblasts in EdU-positive cells. More EdU-positive  
715 cells remained as the neoblasts in *cdhl* KD animals. Data are mean  $\pm$  SEM ( $n = 3$ ; Student's *t*-test, \*  
716  $p < 0.05$ ).  
717



718

719 **Fig. 4 The neoblasts in *cdh1* KD animals did not form differentiating blastema but underwent**  
 720 **activation of ERK signaling.**

721 (A) Expression pattern of *piwiA* in control and *cdh1* KD animals at 3 dpa. *cdh1* KD animals did not  
 722 show differentiating blastema. Scale bars, 500  $\mu$ m. (B) Western blotting of pERK in control and  
 723 *cdh1* KD animals treated with DMSO or 25  $\mu$ M U0126. *cdh1* KD animals showed pERK, like  
 724 control animals, and U0126 effectively inhibited the phosphorylation of ERK in both animals. (C)  
 725 Expression patterns of *mkpA* and *piwiA* in control and *cdh1* KD animals at 1 dpa. *mkpA* was  
 726 expressed in differentiated or differentiating cells in control animals, and U0126 inhibited the  
 727 expression. In contrast, the *mkpA* was expressed in the neoblasts in *cdh1* KD animals. Scale bars, 25  
 728  $\mu$ m. (D) The expression level of *mkpA* in control and *cdh1* KD animals that were either intact or 1  
 729 dpa. The values are relative to those in control animals. The *mkpA* expression was comparable

730 between control and *cdhl* KD animals. Data are mean  $\pm$  SEM (Student's *t*-test, NS: no significant  
731 difference).